Robust Routing for Vehicular Energy Network

Albert Y.S. Lam
Department of Electrical and Electronic Engineering
The University of Hong Kong
Pokfulam Road, Hong Kong
ayslam@eee.hku.hk

James J.Q. Yu
Department of Electrical and Electronic Engineering
The University of Hong Kong
Pokfulam Road, Hong Kong
jqyu@eee.hku.hk

ABSTRACT

The electric vehicle (EV) will become one of the major forms of conveyance for ground transportation in the near future. Due to its intrinsic properties, EV seamlessly bridges the energy and mobility aspects of the smart city. Recently, the vehicular energy network (VEN) has been developed and it is capable of conveying energy over a road network by means of EVs. To do this, certain energy paths need to be properly routed for transmitting energy from an energy source to a destination. However, the establishment of energy paths relies on the underlying vehicular traffic flows, which are generally uncertain when constructing the energy paths. This may lead to infeasible energy routes during implementation. In this paper, we focus on the maximum energy delivery problem of VEN and develop its robust routing design based on robust optimization. We perform a series of simulations to evaluate the effectiveness of the robust routing scheme. We also investigate the sensitivity of the traffic uncertainties and the influence of the number of constructed energy paths. Simulation results show that we can cope with various uncertainties without impairing the energy delivery efficiency significantly.

CCS Concepts

•Networks → Network management; •Hardware → Reusable energy storage; Smart grid;

Keywords

Vehicular energy network; routing; electric vehicles; renewable energy; smart city

e-Energy '17, May 16-19, 2017, Shatin, Hong Kong
 ISBN 978-1-4503-5036-5/17/05…$15.00
DOI: http://dx.doi.org/10.1145/3077839.3078465

1. INTRODUCTION

With the Internet of things and various information and communication technologies, a city can manage its assets in a smarter way, constituting the urban development vision of smart city [13]. This facilitates more efficient use of physical infrastructure and encourages citizen participation. Many governments have been devoting to developing smart cities (nations). Many cities (nations), like Amsterdam, Barcelona, and Singapore, have demonstrated the success of the smart city initiatives.

Based on [16], smart energy and smart mobility are among the key aspects of smart city. The electric vehicle (EV) is believed to take a key role in advancing these technologies. EVs are powered by various energy sources or the electricity grid. With proper scheduling, a large fleet of EVs can get charged from charging stations and parking infrastructures [5]. By replacing the internal combustion engine vehicles with EVs, we can reduce our reliance on fossil fuels and utilize the renewable energy more effectively. The market of EVs is growing very fast and there will likely be an abundance of EVs running on the road in the near future [2]. EVs are also important building blocks to develop intelligent transportation system [9].

Although the battery capacity of a single EV is small, an aggregation of EVs can perform as a significant power source or load, constituting the vehicle-to-grid (V2G) system. Besides acquiring energy from the grid, EVs, in V2G, can also support the grid by providing various demand response [17] and auxiliary services [7]. Many countries have set up future plans for V2G. For example, a large-scale V2G prototype composed of 100 V2G units was launched in the United Kingdom [15]. NREL in the United States works on integrating energy systems, power grid, renewable sources, and EVs to minimize greenhouse gas emissions and other costs [14].

In addition to V2G, EVs can interact with the grid in other formats. Recently, the vehicular energy network (VEN) has been developed [6, 8] and it is capable of transporting a large amount of energy over the road network by means of EVs. Suppose that the road network are equipped with a number of wireless charging facili-

ties, supported by energy storage as buffer, where those EVs running over them can be charged and discharged on the move wirelessly. Consider that an abundance of EVs run along various vehicular routes based on their own schedules. Through appropriate charging and discharging, energy can be disseminated in the road network imperceptibly in the "store-and-forward" manner. With proper routing, energy paths, linked by fragments of vehicular routes, can be constructed to transmit energy from an energy source to a destination with the deliverable energy maximized or the energy loss minimized [10, 11]. VEN can complement the power system by absorbing excessive power from the grid and supplying deficient power to the grid.

The formation for energy paths relies on the traffic in the road network. The existing VEN routing strategies [10, 11] assume static traffic flows, which may not be realistic in most situations. Traffic is generally dynamic such that the energy paths constructed during the planning phase may no longer be optimal, or even become infeasible, for implementation. In this work, we address this issue with robust optimization [3]. We focus on the maximum energy delivery problem (MEDP) of VEN and develop its robust routing scheme. Simulations will show that our robust design can cope with traffic uncertainties without impairing the energy delivery efficiency significantly.

The rest of the paper is organized as follows. Section 2 describes the VEN system model and introduce MEDP. In Section 3, we develop the robust formulation of MEDP. We evaluate the performance of robust routing in Section 4 and conclude in Section 5.

2. SYSTEM MODEL

The system model basically follows [8]. VEN has a layered structure, composed of the underlaying vehicular network and the overlay energy network.

2.1 Vehicular Network

Consider that a fleet of EVs participate in VEN. The vehicular network refers to the system of interconnected roads where EVs traverse based on their individual travel plans. The network is modeled by a directed graph $\mathcal{G}(\mathcal{N}, \mathcal{A})$, where $\mathcal{N}$ and $\mathcal{A}$ are the sets of road junctions and interconnects, respectively. Each arc $a \in \mathcal{A}$ is described by $(tail(a), head(a))$, in which vehicles go along from $tail(a) \in \mathcal{N}$ to $head(a) \in \mathcal{N}$. Certain consecutive arcs form a vehicular route and a particular route r_i with $|r_i|$ arcs is represented by $\langle a^i_1, \ldots, a^i_{|r_i|}\rangle$. We denote the nth arc of r_i by $r_i(n)$ such that $r_i(n) = a^i_n$. We also describe the sub-route connecting $r_i(n)$ and $r_i(m)$ with $r_i(n, m) = \langle a^i_n, \ldots, a^i_m\rangle$. With known traffic, we can determine a set of vehicular routes, denoted by $\mathcal{R}$, for $\mathcal{G}(\mathcal{N}, \mathcal{A})$.

2.2 Energy Network

Suppose that there are a wireless charging facility and an energy buffer storage installed at each $n \in \mathcal{N}$. With dynamic (dis)charging technologies [12], a passing EV can pick up or drop off a "packet" of energy seamlessly at n. We standardize the size of each energy packet by w, which should be sufficiently small. Consider that we decide to transmit a certain amount of energy from $n_s \in \mathcal{N}$ to $n_t \in \mathcal{N}$. We can construct a set of energy paths, denoted by $\mathcal{P}(n_s, n_t)$, over VEN. Each $p_j \in \mathcal{P}(n_s, n_t)$ is linked by $|p_j|$ vehicular sub-routes, i.e., $p_j = \langle r^j_1(n_1, m_1), \ldots, r^j_i(n_i, m_i), \ldots, r^j_{|p_j|}(n_{|p_j|}, m_{|p_j|})\rangle$, where $r^j_i(n_i, m_i)$ is the ith sub-route of p_j. Note that $tail(r^j_1(n_1)) = n_s$ and $head(r^j_{|p_j|}(m_{|p_j|})) = n_s$.

It takes time for a vehicle to go from a place to another. Suppose that it takes $d(a)$ seconds to traverse Arc a on the average. In this sense, to pass through the sub-route $r^j_i(n_i, m_i)$, it incurs an average delay of $d(r^j_i(n_i, m_i)) = \sum_{a \in r^j_i(n_i, m_i)} d(a)$. Since generally several sub-routes make up an energy path, the energy would experience an average propagation delay d_j along Energy Path $p_j(n_s, n_t)$ as

$$d_j \triangleq \sum_{i=1}^{|p_j|} d(r^j_i(n_i, m_i)) = \sum_{i=1}^{|p_j|} \sum_{a \in r^j_i(n_i, m_i)} d(a) = \sum_{a \in p_j} d(a). \quad (1)$$

Let f^j_i be the traffic rate of the ith sub-route of $p_j(n_s, n_t)$ corresponding to the participating EVs. With packet size w, the energy transmission rate g_j of $p_j(n_s, n_t)$ is no larger than wf^j_i for all $i = 1, \ldots, |p_j|$. Hence, for all $r^j_i(n_i, m_i)$ in $p_j(n_s, n_t)$, we have

$$g_j \le w f^j_i. \quad (2)$$

A particular arc a may be shared by multiple energy paths. Let h_a be the aggregate vehicular flow of a. For each a in $\mathcal{A}$, there should be enough EVs supporting the energy transmissions of the energy paths which share a and thus we have

$$\sum_{j | a \in p_j} \frac{g_j}{w} \le h_a. \quad (3)$$

Wireless energy transfer incurs energy loss. Let $0 \le z_c \le 1$ and $0 \le z_d \le 1$ be the charging and discharging efficiencies, respectively. When an EV is wirelessly charged, a fraction $(1 - z_c)$ of energy will be lost. Similarly, discharging results in a fraction $(1 - z_d)$ of energy loss. Along $p_j(n_s, n_t)$, EVs will experience $|p_j|$ times of charging and discharging. Define $z = z_c z_d$. Suppose that x_j units of energy need to reach n_t along $p_j(n_s, n_t)$, we should inject $\frac{x_j}{z^{|p_j|}}$ units of energy at n_s so as to compensate $(\frac{x_j}{z^{|p_j|}} - 1)x_j$ units of energy loss.

Besides the propagation delay, transmitting energy along $p_j(n_s, n_t)$ also requires the transmission delay of

$\frac{x_j}{z^{|p_j|}g_j}$. So the total amount of time required to transfer energy along $p_j(n_s, n_t)$ is $d_j + \frac{x_j}{z^{|p_j|}g_j}$.[1] If T is the time window for energy transmission, the amount of energy transferrable along $p_j(n_s, n_t)$ should be upperly bounded by $(T - d_j)z^{|p_j|}g_j$. Thus we have

$$x_j \leq (T - d_j)z^{|p_j|}g_j. \tag{4}$$

2.3 Energy Delivery Maximization

Consider that we decide to transmit energy from n_s to n_t over $\mathcal{G}(\mathcal{N}, \mathcal{E})$. Without loss of generality, we denote the jth energy paths connecting n_s and n_t by p_j and the whole set of energy paths by $\mathcal{P}$. By the energy path construction method given in [10,11], we can construct $\mathcal{P}$. We are interested in maximizing the total amount of transferable energy subject to an upper bound of total energy loss, given by $\overline{L}$. We can formulate the corresponding deterministic MEDP as follows:

Problem 1 (DETERMINISTIC MEDP).

$$\textit{maximize} \quad \sum_{j|p_j \in \mathcal{P}} x_j \tag{5a}$$

$$\textit{subject to} \quad x_j \leq (T - d_j)z^{|p_j|}g_j, \quad \forall j|p_j \in \mathcal{P}, \tag{5b}$$

$$g_j \leq w f_i^j, \quad \forall i, j|r_i^j(n_i, m_i) \in p_j, p_j \in \mathcal{P}, \tag{5c}$$

$$\sum_{j|a \in p_j} \frac{g_j}{w} \leq h_a, \quad \forall a \in \mathcal{A}, \tag{5d}$$

$$\sum_{j|p_j \in \mathcal{P}} (\frac{1}{z^{|p_j|}} - 1)x_j \leq \overline{L}, \tag{5e}$$

$$x_j \geq 0, g_j \geq 0, \quad \forall j|p_j \in \mathcal{P}, \tag{5f}$$

where x_j and g_j are variables while z, $|p_j|$,T, w, $\overline{L}$, d_j, f_i^j, and h_a are system parameters. Problem 1 is in fact a linear program (LP).

3. ROBUST OPTIMIZATION

Among all parameters, while z, $|p_j|$, T, w, and $\overline{L}$ are determined and fixed by the system, d_j, f_i^j, and h_a are subject to uncertainties due to traffic. In most situations, the values of these traffic-related parameters cannot be known to high accuracy. According to [4], an illustrative example of LP shows that small perturbations of some parameters can make the nominal optimal solution heavily infeasible. Although the problem defined in Section 2.3 is just an LP which can be solved very effectively, the computed solution may not be practically useful or even infeasible when the traffic data are realized.

To address this issue, we model those constraints involving d_j, f_i^j, and h_a in Problem 1 with chance constraints. Let $\beta_j = z^{|p_j|}$. Then we have the following chance constrained optimization problem:

[1]For various kinds of delays experienced in VEN, the interested reader may refer to [8].

Problem 2 (CHANCE CONSTRAINED MEDP).

$$\textit{maximize} \quad \sum_{j|p_j \in \mathcal{P}} x_j \tag{6a}$$

$$\textit{subject to} \quad \Pr\left\{x_j - T\beta_j g_j + \tilde{d}_j \beta_j g_j > 0\right\} \leq \theta_\Delta, \quad \forall j|p_j \in \mathcal{P}, \tag{6b}$$

$$\Pr\left\{g_j > w\tilde{f}_i^j\right\} \leq \theta_\Delta, \quad \forall i, j|r_i^j(n_i, m_i) \in p_j, p_j \in \mathcal{P}, \tag{6c}$$

$$\Pr\left\{\sum_{j|a \in p_j} w^{-1} g_j > \tilde{h}_a\right\} \leq \theta_\Delta, \quad \forall a \in \mathcal{A}, \tag{6d}$$

$$(5e), (5f),$$

where $\tilde{d}_j$, $\tilde{f}_i^j$, and $\tilde{h}_a$ be the uncertain versions of d_j, f_i^j, and h_a, respectively, and $0 \leq \theta_\Delta \leq 1$. Problem 2 is the same as Problem 1 except (6b), (6c), and (6d). (6b) means that we allow a probability of θ_Δ of violating (5b). Similarly, we have (6c) for (5c) and (6d) for (5d).

For each $a \in \mathcal{A}$, we model its uncertain delay as $\tilde{d}(a) = d(a) + \xi(a)\hat{d}(a)$, where $d(a)$, $\xi(a)$, and $\hat{d}(a)$ denote the nominal value of $\tilde{d}(a)$, an independent random variable representing its uncertainty, and its positive constant perturbation, respectively. By (1), the delay of p_j is given as $\tilde{d}_j = \sum_{a \in p_j}[d(a) + \xi(a)\hat{d}(a)]$. For all j such that $p_j \in \mathcal{P}$, we can write the robust counterpart of (6b) as

$$(x_j - T\beta_j g_j + \beta_j g_j \sum_{a \in p_j} d(a)) + \beta_j g_j \sum_{a \in p_j} \xi(a)\hat{d}(a) \leq 0. \tag{7}$$

Similarly, we model the uncertain traffic rate as $\tilde{f}_i^j = f_i^j + \zeta_i^j \hat{f}_i^j$, where f_i^j, ζ_i^j, and $\hat{f}_i^j$ are the nominal value of $\tilde{f}_i^j$, the corresponding independent random variable and perturbation. For all i and j such that $r_i^j(n_i, m_i)$ in p_j and p_j in $\mathcal{P}$, we can represent (6c) as

$$g_j - \zeta_i^j w \hat{f}_i^j \leq w f_i^j. \tag{8}$$

With similar ideas, we model the aggregate traffic flow of Arc a as $\tilde{h}_a = h_a + \varsigma_a \hat{h}_a$, where h_a, ς_a, and $\hat{h}_a$ are the nominal value of $\tilde{h}_a$, the corresponding independent random variable and perturbation. For all $a \in \mathcal{A}$, (6d) gives

$$\sum_{j|a \in p_j} w^{-1} g_j - \varsigma_a \hat{h}_a \leq h_a. \tag{9}$$

We denote the vectors of $\xi(a)$, ζ_i^j, and ς_a by ξ, ζ, and ς. Consider that $[\xi, \zeta, \varsigma]$ are confined in the uncertainty set $\mathcal{U}$. To immunize against infeasibility, we aim to find a feasible solution for any $[\xi, \zeta, \varsigma]$ in $\mathcal{U}$. Consider the notation of $proj_y(\mathcal{U})$ refers to the projection of $\mathcal{U}$ into y. We construct the corresponding set-induced robust optimization problem as follows:

Problem 3 (SET-INDUCED ROBUST MEDP).

$$\textit{maximize} \quad \sum_{j|p_j\in\mathcal{P}} x_j \tag{10a}$$

$$\textit{subject to} \quad (x_j - T\beta_j g_j + \beta_j g_j \sum_{a\in p_j} d(a)) + \sup_{\xi\in proj_\xi(\mathcal{U})} [\beta_j g_j \sum_{a\in p_j} \xi(a)\hat{d}(a)] \le 0, \quad \forall j|p_j\in\mathcal{P}, \tag{10b}$$

$$g_j + \sup_{\zeta\in proj_\zeta(\mathcal{U})} [-\zeta_i^j w\hat{f}_i^j] \le w f_i^j, \quad \forall i,j|r_i^j(n_i,m_i)\in p_j, p_j\in\mathcal{P}, \tag{10c}$$

$$\sum_{j|a\in p_j} w^{-1} g_j + \sup_{\varsigma\in proj_\varsigma(\mathcal{U})} [-\varsigma_a \hat{h}_a] \le h_a, \quad \forall a\in\mathcal{A}, \tag{10d}$$

$$(5e), (5f).$$

We consider the box uncertainty set $\mathcal{U} = \{(\xi,\zeta,\varsigma) \mid |\xi(a)| \le \overline{\xi}, |\zeta_i^j| \le \overline{\zeta}, |\varsigma_a| \le \overline{\varsigma}, \forall a,i,j|a \in r_i^j(n_i,m_i) \in p_j \in \mathcal{P}\}$. Then Problem 3 becomes

Problem 4 (BOX-UNCERTAIN ROBUST MEDP).

$$\textit{maximize} \quad \sum_{j|p_j\in\mathcal{P}} x_j \tag{11a}$$

$$\textit{subject to} \quad (x_j - T\beta_j g_j + \beta_j g_j \sum_{a\in p_j} d(a)) + \beta_j g_j \overline{\xi} \sum_{a\in p_j} \hat{d}(a) \le 0, \quad \forall j|p_j\in\mathcal{P}, \tag{11b}$$

$$g_j + w\overline{\zeta}\hat{f}_i^j \le w f_i^j, \quad \forall i,j|r_i^j(n_i,m_i)\in p_j\in\mathcal{P}, \tag{11c}$$

$$\sum_{j|a\in p_j} w^{-1} g_j + \overline{\varsigma}\hat{h}_a \le h_a, \quad \forall a\in\mathcal{A}, \tag{11d}$$

$$(5e), (5f).$$

4. PERFORMANCE EVALUATION

We evaluate the performance of robust VEN routing with a series of simulations. We first compare the energy delivery performance of robust routing with deterministic routing developed in [10]. Then we investigate the impact of uncertainty bounds of $\overline{\xi}$, $\overline{\zeta}$, and $\overline{\varsigma}$ on the energy delivery efficiency. Finally, we examine the impact of different numbers of energy paths. We perform the simulations on a computer with an Intel Core i7 CPU at 3.60 GHz and 32 GB RAM. The model is coded with Python 3, and the optimization problem is solved by the Gurobi optimization solver [1].

4.1 Robust Optimization Performance

In this test, we study on two grid networks with bi-directional edges: the 16-node and 25-node networks

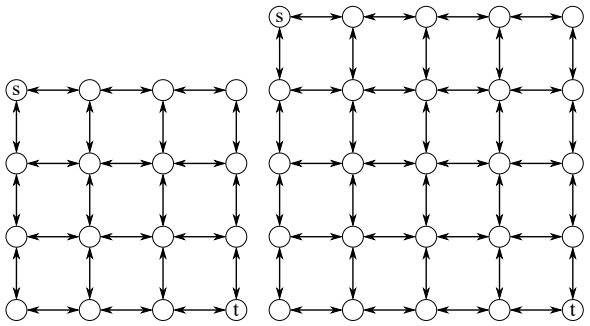

(a) 16-node grid network (b) 25-node grid network

Figure 1: Road network test cases.

given in Fig. 1, where s and t refer to the energy source and destination, respectively. We follow the simulation configurations of [10] to set up the nominal parameter settings. All road connections in the networks are 10 km long and the nominal vehicular speed is set to 60 km/h. Thus vehicles need 600 seconds to run through a road in the network. In both networks, 20 vehicular routes are randomly generated. For the vehicular flow of each route, the EV density is set to 0.1 EVs per second. The energy packet size w is set to 1 kWh and the energy efficiency for each charging-discharging cycle z is 0.9. The test spans for 5 hours, i.e., $T = 14400$ seconds. We assume that the uncertain $\tilde{d}(a)$, $\tilde{f}_i^j$, and $\tilde{h}_a$ may deviate from their nominal values by at most 10%, i.e., $\hat{d}(a) = 0.1d(a)$, $\hat{f}_i^j = 0.1f_i^j$, and $\hat{h}_a = 0.1h_a$. The uncertainty bounds $\overline{\xi}, \overline{\zeta}, \overline{\varsigma}$ are set to one.

We solve the robust Problem 4 and original Problem 1 on both networks with different energy loss limits $\overline{L}$. The simulation results are presented in Tables 1 and 2. It can be observed that the amount of deliverable energy increases with $\overline{L}$, and then converges due to the change of constraint tightness with respect to (1) and (4). When $\overline{L}$ is small, (5e) is the bounding constraint that prevents the improvement of objective function value. However, the other constraints dominate when $\overline{L}$ gets large, which suppresses the impact of $\overline{L}$ on the objective function value.

Moreover, the amount of deliverable energy for (1) and (4) are identical when $\overline{L}$ is small (< 500). Meanwhile, robust optimization achieves slightly smaller deliverable energy with larger $\overline{L}$. This is because in robust optimization (4), the feasible solution space must be reduced to immunize against infeasibility due to the uncertainties. This demonstrates that the robust routing does not impair the energy delivery efficiency significantly while being robust in the presence of uncertainty.

4.2 Sensitivity on Uncertainty bounds

We also investigate the impact of the uncertainty bounds on energy delivery. To assess the maximum

Table 1: Energy Delivery and Loss on 16-node Network

$\overline{L}$	Robust Optimization		Original Optimization	
	Delivery	Loss	Delivery	Loss
1	2.69	1.00	2.69	1.00
100	269.00	100.00	269.00	100.00
200	538.01	200.00	538.01	200.00
500	1221.77	500.00	1259.16	500.00
700	1603.33	700.00	1640.73	700.00
776	1748.33	776.00	1785.72	776.00
777	1750.21	776.99	1787.63	777.00
800	1750.21	776.99	1831.51	800.00
885	1750.21	776.99	1993.67	885.00
886	1750.21	776.99	1994.54	885.46
1000	1750.21	776.99	1994.54	885.46

Table 2: Energy Delivery and Loss on 25-node Network

$\overline{L}$	Robust Optimization		Original Optimization	
	Delivery	Loss	Delivery	Loss
1	2.69	1.00	2.69	1.00
100	269.00	100.00	269.00	100.00
200	538.01	200.00	538.01	200.00
500	1196.59	500.00	1233.72	500.00
700	1578.15	700.00	1615.29	700.00
703	1583.87	703.00	1621.01	703.00
704	1585.66	703.94	1622.92	704.00
800	1585.66	703.94	1806.07	800.00
811	1585.66	703.94	1827.06	811.00
812	1585.66	703.94	1828.33	811.67
1000	1585.66	703.94	1828.33	811.67

Table 3: Sensitivity of Maximum Energy Delivery on Unvertainty Bounds

$\overline{\varsigma}$	$\overline{\zeta}$	$\overline{\xi}$				
		0.2	0.5	1.0	2.0	5.0
0.2	5	1944.88	1930.22	1905.79	1856.92	1710.32
0.2	6	1930.42	1915.34	1890.20	1840.76	1695.44
0.2	7	1914.36	1898.81	1872.88	1822.81	1678.91
0.2	8	1879.50	1863.61	1837.13	1786.91	1645.84
0.2	9	1816.45	1801.57	1776.78	1729.07	1592.56
0.5	5	1885.34	1871.13	1847.45	1800.08	1657.96
0.5	6	1873.30	1858.73	1834.46	1786.61	1645.56
0.5	7	1857.24	1842.20	1817.13	1768.66	1629.03
0.5	8	1825.51	1810.11	1784.46	1735.75	1598.72
0.5	9	1762.87	1748.39	1724.27	1677.91	1545.44
1.0	5	1786.11	1772.65	1750.21	1705.34	1570.70
1.0	6	1778.08	1764.38	1741.55	1696.36	1562.44
1.0	7	1762.02	1747.85	1724.23	1678.41	1545.90
1.0	8	1735.52	1720.95	1696.67	1650.49	1520.18
1.0	9	1673.56	1659.76	1636.76	1592.64	1466.91
2.0	5	1587.66	1575.69	1555.74	1515.85	1396.18
2.0	6	1587.66	1575.69	1555.74	1515.85	1396.18
2.0	7	1571.60	1559.16	1538.42	1497.90	1379.65
2.0	8	1555.53	1542.62	1521.10	1479.95	1363.11
2.0	9	1494.95	1482.50	1461.74	1422.11	1309.84
5.0	5	992.29	984.81	972.34	947.41	872.61
5.0	6	992.29	984.81	972.34	947.41	872.61
5.0	7	992.29	984.81	972.34	947.41	872.61
5.0	8	984.25	976.54	963.68	938.43	864.35
5.0	9	957.75	949.64	936.12	910.51	838.63

amount of deliverable energy through robust routing, we nullify the bounding impact of energy loss by setting $\overline{L} = \infty$. In this case, the change of the result is mainly contributed by the uncertainty bounds. The simulation settings follows Section 4.1 except for $\overline{\xi}$, $\overline{\zeta}$, and $\overline{\varsigma}$, whose values are set to $[0.2, 0.5, 1.0, 2.0, 5.0]$, $[5, 6, 7, 8, 9]$[2], and $[0.2, 0.5, 1.0, 2.0, 5.0]$, respectively. 125 combinations of these three bounds are tested on the 16-node grid network and the results are presented in Table 3. The larger uncertainty bounds, the less energy can be delivered. The results accords with the intuition that the routing scheme must be feasible for all possible random cases within the undertainty set $\mathcal{U}$. In addition, we can observe that the robust optimization is more sensitive to $\overline{\varsigma}$ than to $\overline{\xi}$ while $\overline{\zeta}$ only asserts a small influence. This is due to the fact that in Problem 4, (11d) is the bounding constraint in most cases when (5e) is relaxed.

4.3 Subset of Energy Paths

In the previous tests, the small testing networks allow us to enumerate all energy paths for optimization. However, in most real-world scenarios, the vehicular road network and traffic conditions are so complicated such that it is intractable and inefficient to construct all energy paths. Thus only a subset of energy paths can be employed. In this test, we assess the performance of robust routing on a large grid network with 100 nodes, in which only a small subset of energy paths are utilized. The simulation configurations are identical to those used Section 4.1, and the top left and bottom right nodes are considered as source and destination, respectively. Energy paths of quantity of $[100, 200, 500, 1000, 1500, 2000]$ are randomly generated and the maximum deliverable energy with respect to various energy loss limits are examined. The simulation results are depicted in Fig. 2.

We can see that the number of energy paths has a significant influence on the maximum energy delivery when $\overline{L}$ is not limiting. In general, VEN can deliver more energy with more energy paths until it is saturated at a threshold (1500 in most our cases). The reason is that while each additional energy path provides extra energy delivery capacity, it still relies on the underlying EV traffic flow, which is limited. When many energy paths are employed, multiple energy paths are likely to share some of the road connections, in which the passing EVs are shared by these paths.

Moreover, when $\overline{L}$ involves in the bounding constraint ($\overline{L} < 1000$ in this case), the number of energy paths still influences the performance. The more energy paths, the larger amount of energy can be delivered. This is due to the fact that more energy paths can provide more options for energy transmission and the energy efficient paths with less charging-discharging cycles are more likely to be active.

[2]The results are the same when $\overline{\zeta} \leq 5$. So we only give those results with $\overline{\zeta} \geq 5$.

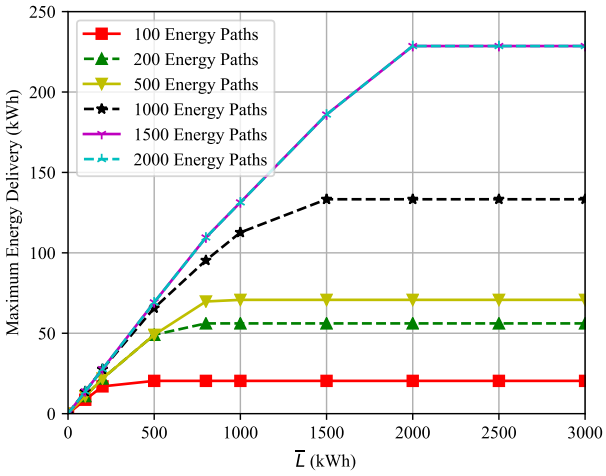

Figure 2: Maximum energy delivery with different number of energy paths utilized.

5. CONCLUSION

The increasing demands of EVs and the various mature peripheral technologies facilitate the development of VEN, in which a large amount of energy can be transmitted over the vehicular network by means of EVs. To transmit energy between an energy source and a destination, energy paths need to be developed. The previous VEN routing techniques assume static vehicular traffic flows, which cannot be known to high accuracy in the planning process. The resultant energy paths may also be infeasible when the traffic data are realized. To overcome this, we consider uncertain traffic flows and develop robust routing for VEN. We focus on maximum energy delivery and formulate the robust MEDP. We conduct a series of simulations to evaluate the effectiveness of the robust routing scheme. Simulation results confirm that the robust routing strategies can manage the traffic uncertainties and the energy delivery efficiency is not impaired significantly.

6. ACKNOWLEDGMENTS

This research is supported in part by the Theme-based Research Scheme of the Research Grants Council of Hong Kong, under Grant No. T23-701/14-N.

7. REFERENCES

[1] Gurobi Optimization. http://www.gurobi.com/.

[2] Electric vehicles market by vehicle – growth, share, opportunities & competitive analysis, 2016 – 2022. Technical Report 57989-07-16, Credence Research, Jul. 2016.

[3] A. Ben-Tal, L. El Ghaoui, and A. S. Nemirovski. *Robust Optimization*. Princeton University Press, Princeton, NJ, 2009.

[4] A. Ben-Tal and A. Nemirovski. Robust solutions of linear programming problems contaminated with uncertain data. *Math. Program., Ser. A*, 88:411–424, Oct. 2000.

[5] L. Gan, U. Topcu, and S. H. Low. Optimal decentralized protocol for electric vehicle charging. *IEEE Trans. Power Syst.*, 28(2):940–951, May 2013.

[6] A. Y. S. Lam, K.-C. Leung, and V. O. K. Li. An electric-vehicle-based supplementary power delivery system. In *Proc. 6th IEEE Int. Conf. on Smart Grid Comm.*, pages 307–312, Miami, FL, Nov. 2015.

[7] A. Y. S. Lam, K.-C. Leung, and V. O. K. Li. Capacity estimation for vehicle-to-grid frequency regulation services with smart charging mechanism. *IEEE Trans. Smart Grid*, 7(1):156–166, Jan. 2016.

[8] A. Y. S. Lam, K.-C. Leung, and V. O. K. Li. Vehicular energy network. *IEEE Trans. Transport. Electrific.*, to appear, 2017.

[9] A. Y. S. Lam, Y.-W. Leung, and X. Chu. Autonomous vehicular public transportation system: Scheduling and admission control. *IEEE Trans. Intell. Transp. Syst.*, 17(5):1210–1226, May 2016.

[10] A. Y. S. Lam and V. O. K. Li. Opportunistic routing for vehicular energy network. *Submitted for publication.*

[11] A. Y. S. Lam and V. O. K. Li. Energy loss minimization for vehicular energy network routing. In *Proc. ACM Workshop on Electric Vehicle Systems, Data, and Applications*, Waterloo, Canada, Jun. 2016.

[12] F. Lu, H. Zhang, H. Hofmann, and C. C. Mi. A dynamic charging system with reduced output power pulsation for electric vehicles. *IEEE Trans. Ind. Electron.*, 63(10):6580–6590, Oct. 2016.

[13] S. P. Mohanty, U. Choppali, and E. Kougianos. Everything you wanted to know about smart cities: The internet of things is the backbone. *IEEE Consum. Electron. Mag.*, 5(3):60–70, Jul. 2016.

[14] National Renewable Energy Laboratory. Electric vehicle grid integration, Mar. 2017.

[15] Nissan Newsroom UK. Nissan and enel launch groundbreaking vehicle-to-grid project in the UK, May 2016.

[16] S. Singh. Smart cities – a $1.5 trillion market opportunity. *Forbes*, Jun. 2014.

[17] M. Zeng, S. Leng, S. Maharjan, S. Gjessing, and J. He. An incentivized auction-based group-selling approach for demand response management in V2G systems. *IEEE Trans. Ind. Informat.*, 11(6):1554–1563, Dec. 2015.